

# Retrieval-Enhanced Visual Prompt Learning for Few-shot Classification

Jintao Rong<sup>‡,†</sup> Hao Chen<sup>†</sup> Tianxiao Chen<sup>‡</sup> Linlin Ou<sup>‡</sup> Xinyi Yu<sup>‡</sup> Yifan Liu<sup>\*</sup>

<sup>‡</sup>Zhejiang University of Technology <sup>†</sup>Zhejiang University <sup>\*</sup>The University of Adelaide

## Abstract

*Prompt learning has become a popular approach for adapting large vision-language models, such as CLIP, to downstream tasks. Typically, prompt learning relies on a fixed prompt token or an input-conditional token to fit a small amount of data under full supervision. While this paradigm can generalize to a certain range of unseen classes, it may struggle when domain gap increases, such as in fine-grained classification and satellite image segmentation. To address this limitation, we propose Retrieval-enhanced Prompt learning (RePrompt), which introduces retrieval mechanisms to cache the knowledge representations from downstream tasks. We first construct a retrieval database from training examples, or from external examples when available. We then integrate this retrieval-enhanced mechanism into various stages of a simple prompt learning baseline. By referencing similar samples in the training set, the enhanced model is better able to adapt to new tasks with few samples. Our extensive experiments over 15 vision datasets, including 11 downstream tasks with few-shot setting and 4 domain generalization benchmarks, demonstrate that RePrompt achieves considerably improved performance. Our proposed approach provides a promising solution to the challenges faced by prompt learning when domain gap increases. The code and models will be available.*

## 1. Introduction

Visual concept recognition has achieved remarkable success in a closed set with a large-scale training set, typically the ImageNet dataset. The recognition accuracy can even outperform human ability. However, a large training set for each visual concept may not always be accessible for specific downstream tasks. How to learn a robust visual concept recognition system with low-shot data has become a challenging but valuable problem in computer vi-

sion. Previous methods [10, 42, 45] mainly focus on learning a transferable visual representation from a source domain and quickly adapting to few-shot downstream tasks through fine-tuning techniques. However, limited by the categories and closed set training samples in the source domain, these few-shot learning algorithms only work for impractically simple settings, such as distinguishing 5-way 1-shot classification.

Recently, large-scale vision-language models, such as CLIP [38] and ALIGN [16], have shown promising results in visual representation learning. The feasibility of applying these visual language models to more challenging low-shot learning problems has drawn much attention [54, 33, 21]. CoOP [54] first proposes a few-shot setting to evaluate the performance of visual language models, where there are full  $C$  classes from the downstream tasks and each class has 1/2/4/8/16-shot samples. Meanwhile, CoOP designs a learnable text prompt to replace the sub-optimal hand-crafted text prompt templates. However, the frozen image feature representation of CLIP also leads to sub-optimal performance. Inspired by VPT [17], many studies [50, 25, 48] consider adding extra learnable visual tokens into the image encoder to adequately fine-tune the vision-language models on downstream tasks.

Despite significant improvements achieved by these methods for few-shot, such parametric models struggle to generalize to extremely low-shot data or atypical instances through rote memorization. For instance, when given 1 image for each class, CoOP performs even worse than zero-shot classification results of CLIP. Recent retrieval-augmentation approaches [32, 3, 5, 11, 49, 51] retrieve knowledge corpus to generate addition references for improving performance in low-resource scenarios. Inspired by these approaches, we consider augmenting the prompt learning by retrieving relevant images that are most similar to the overall features of the current image in few-shot training set.

In this work, we propose a Retrieval-enhanced Prompt learning (RePrompt) by introducing the retrieval mechanism to perform associate learning on knowledge representations from downstream tasks. Firstly, RePrompt estab-

Work was done when J. Rong was visiting Zhejiang University. Xinyi Yu are the corresponding authors.

lishes a retrieval database to store common training image representations as retrieval keys. The current image representations query the database to obtain related cached knowledge. In order to integrate the retrieved knowledge into prompt learning, we consider two enhanced strategies depending on the nature of the retrieved value. When the value is the common training image representation, we insert retrieval-enhanced visual prompts into the input of multiple layers of image encoder, where we dynamically learn the retrieval-enhanced visual prompts on retrieved values. When the value is the label, an adapter based on the parametric  $k$ -NN classifier is applied to predict a classification results, which is linearly interpolated into the prediction of the model with retrieval-enhanced prompts. For the trade-off between these strategies, we use a non-parametric  $k$ -nn algorithm between the query instance and the database to obtain a prior-distribution-based loss for guiding the training process. RePrompt achieves leading performance across 11 datasets under various few-shot settings, including the challenging datasets (e.g., ImageNet). Moreover, superior performance on 4 domain generalization benchmarks also demonstrating the generalization ability of our RePrompt for unseen domains.

In summary, the main contributions of this work include:

- We explore the feasibility of introducing retrieval system to augment the prompt learning for vision language models, with a focus on downstream few-shot image classification.
- We propose RePrompt, which establishes a retrieval database from training examples and implements retrieval-enhanced mechanisms in the model input, middle layers, output, and training process.
- The proposed RePrompt achieved state-of-the-art performance over 11 vision datasets under various few-shot settings. It also demonstrates superior performance on 4 domain generalization benchmarks.

## 2. Related Work

**Retrieval-augmented models.** In recent years, retrieval-augmented models have gained significant attention in Natural Language Processing (NLP) and Computer Vision (CV) research fields. In NLP, retrieval-based techniques have been successfully applied to various tasks such as question answering [11, 22, 23], auto-regressive language modeling [3, 5], and other language generation tasks [29]. In the field of CV, retrieval-based approaches have been utilized for Long-tail image classification, image captioning, and image generation [32, 49, 1]. Some semi-parametric methods [35, 24, 23, 51], such as Tip-adapter[51], have also investigated a  $k$ -nearest neighbor(kNN) classifier[2] with an external knowledge storage database to enhance pre-trained models without fine-tuning.

Motivated by the success of retrieval-based methods, we propose a retrieval-based enhancement framework for few-shot classification and domain generalization. Unlike these studies, we focus on retrieving examples from the few-shot training data for constructing a more dynamic prompt that better suited for downstream tasks. The employed kNN classifier similarly benefits from improved visual features, resulting in better classification predictions.

**Parameter-efficient Transfer Learning.** Parameter-efficient Transfer Learning (PETL) [30, 28, 54, 33, 17, 51, 52, 50, 25, 19] has recently become an active research topic due to the rapid growth of pre-trained models. PETL is a fine-tuning approach that aims to fine-tune only a few lightweight modules in the large pre-trained model, thereby matching the performance of fully fine-tuning the model. PETL is first applied in the NLP community to fine-tune large pre-trained models[30, 28]. and has since been applied to large-scale vision and vision-language pre-training models for downstream vision tasks [54, 17]. Two mainstream paradigms of PETL methods include adapter-based approaches [51, 18, 19], which insert lightweight MLP networks to adapt downstream tasks, and prompt-tuning-based methods [54, 53, 33, 17, 50, 25], which add learnable tokens in the input space to bridge the gap between the distribution of training and downstream data. NOAH [52] identifies the optimal configuration of various PETL methods by neural architecture search.

In this work, we propose a dual prompt learning method for the vision-language model, called RePrompt, where we retrieve  $k$  most similar samples to generate visual prompts that are diverse while having a degree of semantic consistency. Moreover, we construct a retrieval-based differentiable adapter to refine the final prediction.

## 3. VLPT: Proposed Prompt Learning Baseline

In this section, we propose a simple dual-modal prompt tuning baseline for the few-shot image classification task, called vision-language prompt tuning (VLPT). VLPT learns visual and text prompts for image encoder and text encoder from few-shot training data simultaneously. The visual prompt is learned by **visual prompt tuning**, while the text prompt is learned by **text prompt tuning**. After deriving image features and text features of categories, the model with tuned prompts generates the prediction following the paradigm of zero-shot classification of CLIP.

**CLIP** [38] is a vision-language pretrained model comprising two sub-networks: an image encoder  $e_I$  and a text encoder  $e_T$ . These encoders encode the visual and text inputs, respectively, into a joint hidden space  $\mathbb{R}^d$ , where vision semantics and language modalities are well-aligned [54]. Here,  $d$  is the dimension of embeddings (e.g.,  $d = 512$  for ViT [8]). For an image  $x$  and a set of  $C$  category names  $T = \{t_1, t_2, \dots, t_C\}$  (e.g.,  $C = 1000$  for Im-

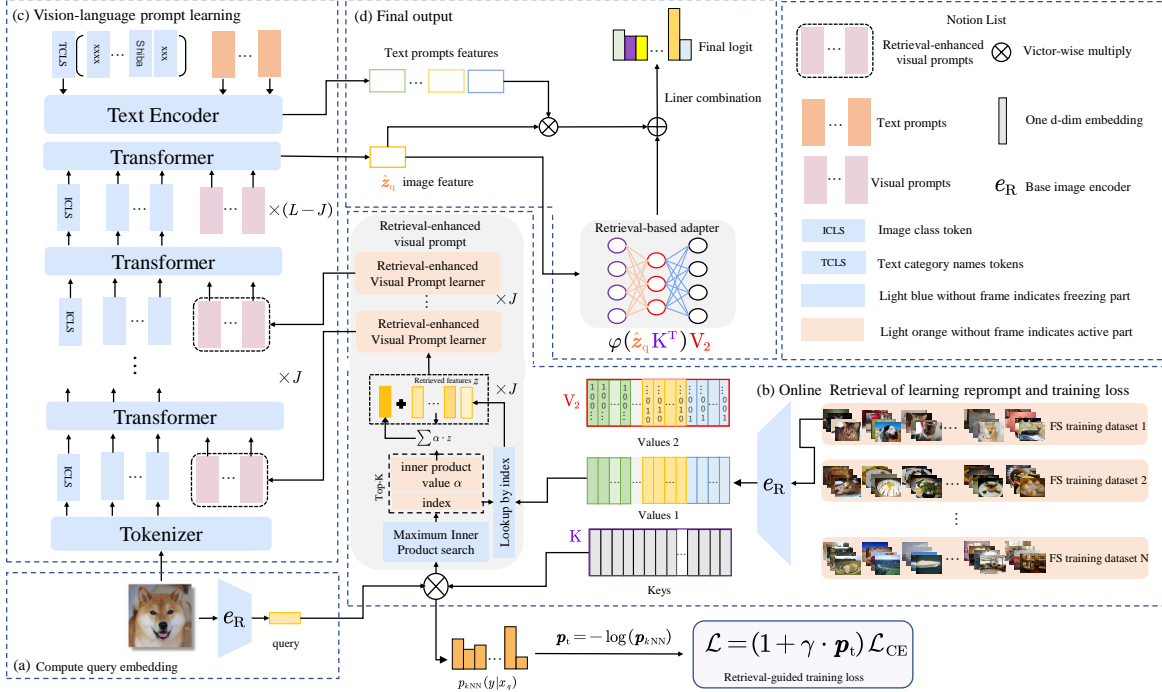


Figure 1. **The overall workflow of RePrompt** comprises four main steps. (a) encode an image input into a query embedding by a frozen base image encoder; (b) encode each image entry from the training dataset into key and value embedding pairs by the same frozen image encoder. Moreover, values also include one-hot representations of labels. We retrieve top-K relevant knowledge items by performing maximum inner product search, and fuse these knowledge as conditions to generate visual prompts. (c) retrieval-enhanced visual prompts are introduced into the  $J$  layers inputs of visual branch, while the remaining prompts are consistent with those of the baseline VLPT.(d) The final output is obtained by a liner combination of the prompt-tuned clip prediction and the retrieval-based adapter prediction.

geNet [7]), the image encoder extracts the image feature  $z = e_I(x) \in \mathbb{R}^d$ . The category names in  $T$  are jointed with a hand-crafted text prompt template a photo of a [CLASS] as text descriptions. The descriptions are further fed into the text encoder to derive the text features  $f \in \mathbb{R}^{d \times C}$ . The prediction probability of  $x$ , belonging to class  $c$ , is calculated by the inner product similarity of query image feature  $z$  and text features  $f$ .

In practice, it is cumbersome to fine-tune the entire vision-language model for transfer learning in each downstream task. Additionally, tuned models suffer from catastrophic forgetting [26, 44], performing poorly on new tasks where the pre-trained model initially performs well. Thus we need a transfer strategy without additional fine-tuning.

**Text prompt learning.** Unlike hard-craft prompt engineering in NLP, text prompt learning consider generating more adaptive text features by learning a set of prompt. CoOp [54] learns a set of parameters  $P_T \in \mathbb{R}^{d \times M}$  to replace the hand-crafted prompt template, where  $M$  is the prompt length. The word token of each category name in  $T$  is filled into a template of  $P_T$  and considered as initial values of learnable input prompts. These prompts are further fine-tuned on few-shot data to generate text features  $f_t$ . The fine-tuned prompt  $P_T$  adjusts the decision boundaries

of text features for downstream tasks. In this process, all parameters inherited from the pre-trained CLIP model are frozen during the training process.

**Visual prompt learning.** VPT [17] proposes a visual prompt tuning approach that introduces a few learnable parameters into the input space while freezing the image encoder  $e_I$  to extract more transferable visual features from downstream data. In the context of image encoding with  $L$  layers, the  $i$ -th layer output  $l_i$ , where  $i = 1, 2, \dots, L$ , can be expressed as:

$$[c, z_1^{i+1}, \dots, z_S^{i+1}] = l_i(c, z_1^i, \dots, z_S^i), \quad (1)$$

where  $c \in \mathbb{R}^d$  denotes the classification token.  $Z^i = \{z_1, \dots, z_S\} \in \mathbb{R}^{d \times S}$  represents a set of input image patch tokens of the  $i$ -th layer, with length  $S$ . Furthermore, the learnable visual prompt  $P_1 \in \mathbb{R}^{d \times N}$ , where  $N$  is the length of visual prompt, is introduced into the input sequence of the  $i$ -th layer, which is following as:

$$[c, \dots, Z^{i+1}] = l_i(c, P_1^i, Z^i). \quad (2)$$

There are two visual prompt variants, VPT-Shallow and VPT-Deep. In the VPT-Shallow approach, the class token  $c$  jointed with image patch tokens and visual prompts is taken

as the input of the first layer, while VPT-Deep inserts independent visual prompts into each layer.

Existing prompt approaches for vision-language models tend to focus on either visual or text prompt learning, ignoring the flexibility of prompt learning in dual-encoders. Moreover, prompt learning approaches may not generalize well on atypical examples due to fully-supervised training with learnable parameters in low-data resource settings. Considering the characteristics of recognition tasks and the flexibility of visual prompt learning, we introduce retrieval and association mechanisms in visual prompt learning to improve the performance.

## 4. Retrieval-enhanced prompt tuning

In this section, we elaborate the proposed Retrieval-enhanced Prompt Tuning for VLPT in detail. RePrompt leverages the retrieval of relevant information from the training dataset (4.1) to enhance the prompt tuning. Figure 1 illustrates the overall workflow of RePrompt, which comprises the vision-language prompt tuning baseline (3) and three retrieval-enhanced modules, retrieval-enhanced visual prompt (4.2), retrieval-based adapter (4.4), and retrieval-guiding training (4.3).

### 4.1. Retrieval module

To fully leverage the existing pretrained model, we utilize a frozen image encoder  $e_R$  to derive the query image feature  $z_q \in \mathbb{R}^d$ . Note that  $e_R$  is a frozen image encoder by vision-language pre-training model. We use the retrieval database act as a robust token repository changing as downstream tasks change. Please refer to supplementary materials for detailed visualization for demonstrating the necessity of using these models as encoders, compared with supervised learning models. Our Retrieval module consists of two steps: (1) building the database, (2) retrieval.

**Retrieval database.** The database is constructed by features extracted from the few-shot training dataset  $\mathcal{D}$ . Specifically, there are  $|\mathcal{D}|$  key-value pairs  $(k_i, v_i)$  in the retrieval database. The key  $k_i = e_R(x_i) \in \mathbb{R}^d$  is the frozen training image representation extracted by  $e_R$ . There are two types of value  $v_i$ , the label  $y \in \mathbb{N}^*$  and the image representation  $z_i = e_R(x_i) \in \mathbb{R}^d$ .

**Effective and efficient retrieval.** As shown in Figure 1, the retrieval database is a matrix  $D \in \mathbb{R}^{|\mathcal{D}| \times d}$  as the fast approximate  $k$ -NN of examples.  $e_R$  produce the query vector  $z_q = e_R(x_q)$  for a query image  $x_q$ . We utilize the query vector  $z_q$  to retrieval its approximate  $k$ -nearest neighbours with corresponding representations  $z_1, z_2, \dots, z_k$  over the matrix  $D$  using cosine similarity. For the retrieval process, we select FAISS [20] to query the database efficiently.

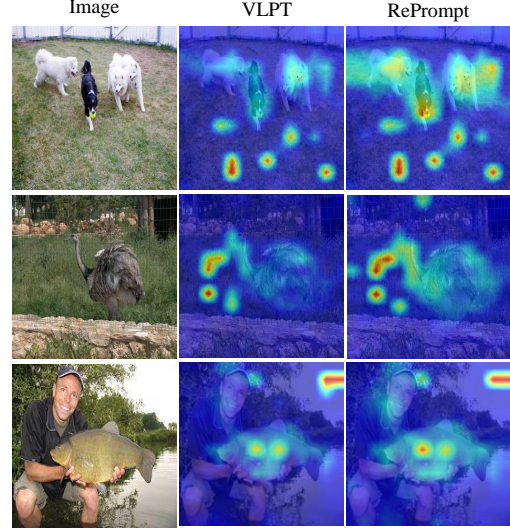


Figure 2. Visualization of attention response map between retrieval-enhanced visual prompts and image patch tokens. The mean self-attention map are from the last vision transformer layers.

### 4.2. Retrieval-enhanced visual prompt

The proposed method aims to enhance visual prompt learning by using a retrieval database for analogy learning. We design to use retrieved results to conditionally generate visual prompts, referred to as retrieval-enhanced visual prompts. The visualization of cross-attention response map of retrieval-enhanced visual prompts and image patch tokens is shown in Figure 2. RePrompt shows stronger self-attention responses, e.g., interesting region expansion and higher attention values.

The retrieval module takes a query vector  $z_q$  from a raw image  $x_q$  and performances a lookup on the matrix  $D$ , returning the top  $k_{re}$  most similar candidates. The corresponding representations  $z_1, z_2, \dots, z_{k_{re}}$  from database are incorporated into the image encoder to augment visual prompts. We intuitively aggregate  $k_{re}$  adjacent representations based on their similarity as an additional fusion vectors  $z_f \in \mathbb{R}^d$  [5] as follows:

$$z_f = \sum_{i=1}^{k_{re}} \alpha_i \cdot z_i; \alpha_i = \frac{e^{z_q \cdot z_i}}{\sum_{i=1}^k e^{z_q \cdot z_i}}. \quad (3)$$

The query vectors  $z_q$ , the fusion vectors  $z_f$  and retrieved vectors  $z_1, z_2, \dots, z_{k_{re}}$  are concatenated to form the input  $\hat{i} = [z_q, z_f, z_1, \dots, z_{k_{re}}] \in \mathbb{R}^{d \times (k_{re}+2)}$  to the visual prompt learner, which generates the retrieval-enhanced visual prompts  $f_p(\hat{i}) \in \mathbb{R}^{d \times (k_{re}+2)}$ .

As illustrated in the top of Figure 3, the visual prompt learner randomly initialize  $J$  visual prompt sets  $P_1^1, \dots, P_1^J$ . Then  $J$  retrieval-enhanced convolution (RE-Conv) blocks are utilized to process  $J$  inputs  $\hat{i}_1, \dots, \hat{i}_J$

(copy  $\hat{\mathbf{i}}$  for  $J$  times) to generate dynamic prompts. These prompts are then combined with  $J$  visual prompts sets separately and inserted into input sequences of the first  $J$  layers of the visual branch:

$$\left[ \mathbf{c}, \dots, \mathbf{Z}^{j+1} \right] = l_j \left( \left[ \mathbf{c}, f_p \left( \hat{\mathbf{i}}_j \right) + \mathbf{P}_I^j, \mathbf{Z}^j \right] \right), j = 1, \dots, J. \quad (4)$$

$12 - J$  layers process remaining input learnable prompts and leaning these prompts degenerates to Equation 2. We further discuss the choice of insertion depth in the supplementary material.

To effectively and efficiently fuse the retrieved representations, we propose a retrieval-enhanced convolution block (REConv). As illustrated in the bottom of Figure 3, a REConv block consists of three convolution layers: two  $1 \times 1$  convolutions that respectively reduce and scale the channel dimensionality and a  $3 \times 3$  convolution that is located in the middle of two  $1 \times 1$  convolutions. Before these convolution layers, we reshape the 1D token sequence structure of visual prompts to the 2D matrix structure. REConv blocks process  $\hat{\mathbf{i}}$  in parallel to generate dynamic prompts, which can be formulated as

$$f_p \left( \hat{\mathbf{i}}_j \right) = \beta \cdot \text{REconv}_j \left( \text{LN} \left( \hat{\mathbf{i}}_j \right) \right) + \hat{\mathbf{i}}_j, j = 1, \dots, J. \quad (5)$$

where LN is Layer Normalization and  $\beta$  is a hyperparameter for scaling the output. More design discussions on handling retrieved representations can be found in the supplementary materials.

### 4.3. Retrieval-based adapter

Furthermore, we use a differentiable  $k$ NN classifier as the retrieval-based adapter. This adapter is trained in conjunction with the retrieval-enhanced visual prompt to generate more adaptive prediction probabilities for downstream tasks. Specifically, given a query instance  $\mathbf{x}_q$ , the query vector  $\hat{\mathbf{z}}_q$  is extracted using the image encoder with retrieval-enhanced visual prompt and lookup on the matrix  $\mathbf{D}$ . The retrieval process returns  $|\mathcal{D}|$ -nearest neighbors with corresponding inner product similarities. Then we aggregate probability mass for each label  $\mathbf{y}_i$  across all its occurrences in the retrieved targets. Suppose  $\mathbf{p}_{k\text{NN}}$  represents the probability of the query instance  $\mathbf{x}_q$  being predicted as  $\mathbf{y}$ , then  $\mathbf{p}_{k\text{NN}}(\mathbf{y}|\mathbf{x}_q)$  is reformulated by weighting sum of the  $\mathbf{p}_{k\text{NN}}$  as following:

$$\mathbf{p}_{k\text{NN}}(\mathbf{y}|\mathbf{x}_q) = \sum_{(\mathbf{z}_i, \mathbf{y}_i) \in \mathcal{D}} \mathbf{1}_{\mathbf{y}=\mathbf{y}_i} \exp((\hat{\mathbf{z}}_q \cdot \mathbf{z}_i)). \quad (6)$$

Furthermore, the  $\mathbf{p}(\mathbf{y}|\mathbf{x}_q)$  is reformulated by interpolating the  $\mathbf{p}_{k\text{NN}}(\mathbf{y}|\mathbf{x}_q)$  with the prediction  $\mathbf{p}_P(\mathbf{y}|\mathbf{x}_q)$  of the prompt-tuning CLIP to get the final probability of the label:

$$\mathbf{p}(\mathbf{y}|\mathbf{x}_q) = \lambda \mathbf{p}_{k\text{NN}}(\mathbf{y}|\mathbf{x}_q) + (1 - \lambda) \mathbf{p}_P(\mathbf{y}|\mathbf{x}_q). \quad (7)$$

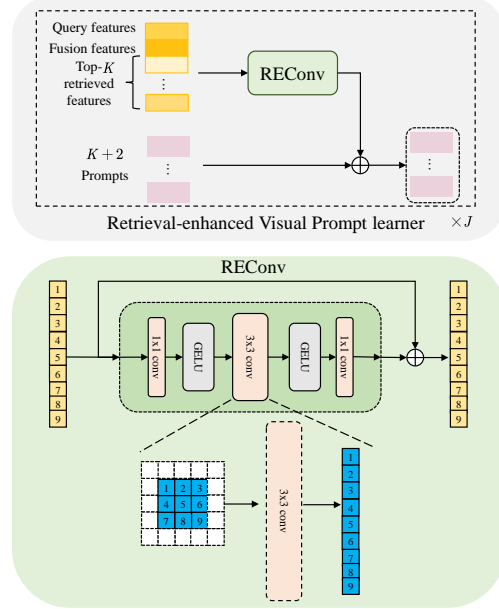


Figure 3. **Overview of visual prompt learner and REConv.** a Visual prompt learner comprises the REConv to generate dynamic visual prompts by learning on retrieved results

Previous semi-parametric few-shot classification work Tip-Adapter-F [51] is similar to our proposed paradigm. **The main difference** is that our query features are derived from the CLIP image encoder branch with retrieval-enhanced prompt. This makes query image features more suitable for the downstream dataset to achieve superior performance to the Tip-Adapter.

### 4.4. Retrieval-guiding training

The  $k$ -nearest neighbor ( $k$ NN) is primarily concerned with the approximation neighborhoods of query instances [2]. It is intuitive to leverage  $k$ NN classification results as prior knowledge to guide RePrompt focus on hard examples during training process. Hard samples usually refer to atypical samples with low confidence. To compute a local probability distribution, we limit the number of samples within the retrieved neighbor set  $\mathbf{K} \subseteq \mathcal{D}$ , where  $k_{rc} \neq |\mathbf{K}|$ , following as:

$$\mathbf{p}_{k\text{NN}}(\mathbf{y}|\mathbf{x}_q) = \sum_{(\mathbf{z}_i, \mathbf{y}_i) \in \mathbf{K}} \mathbf{1}_{\mathbf{y}=\mathbf{y}_i} \exp((\mathbf{z}_q \cdot \mathbf{k}_i)). \quad (8)$$

The probability  $\mathbf{p}_{k\text{NN}}$  corresponds to the confidence of classifying the query instance  $\mathbf{x}_q$  into specific categories. Similar to Focal Loss [31], the negative log-likelihood value of  $\mathbf{p}_{k\text{NN}}$  is used as the adjustment factor  $\mathbf{p}_t = -\log(\mathbf{p}_{k\text{NN}})$ . The adjustment factor reweights the cross-entropy loss  $\mathcal{L}_{\text{CE}}$  by adjusting the relative loss of the pseudo-correct samples or pseudo-error samples distinguished by  $k$ NN. The final

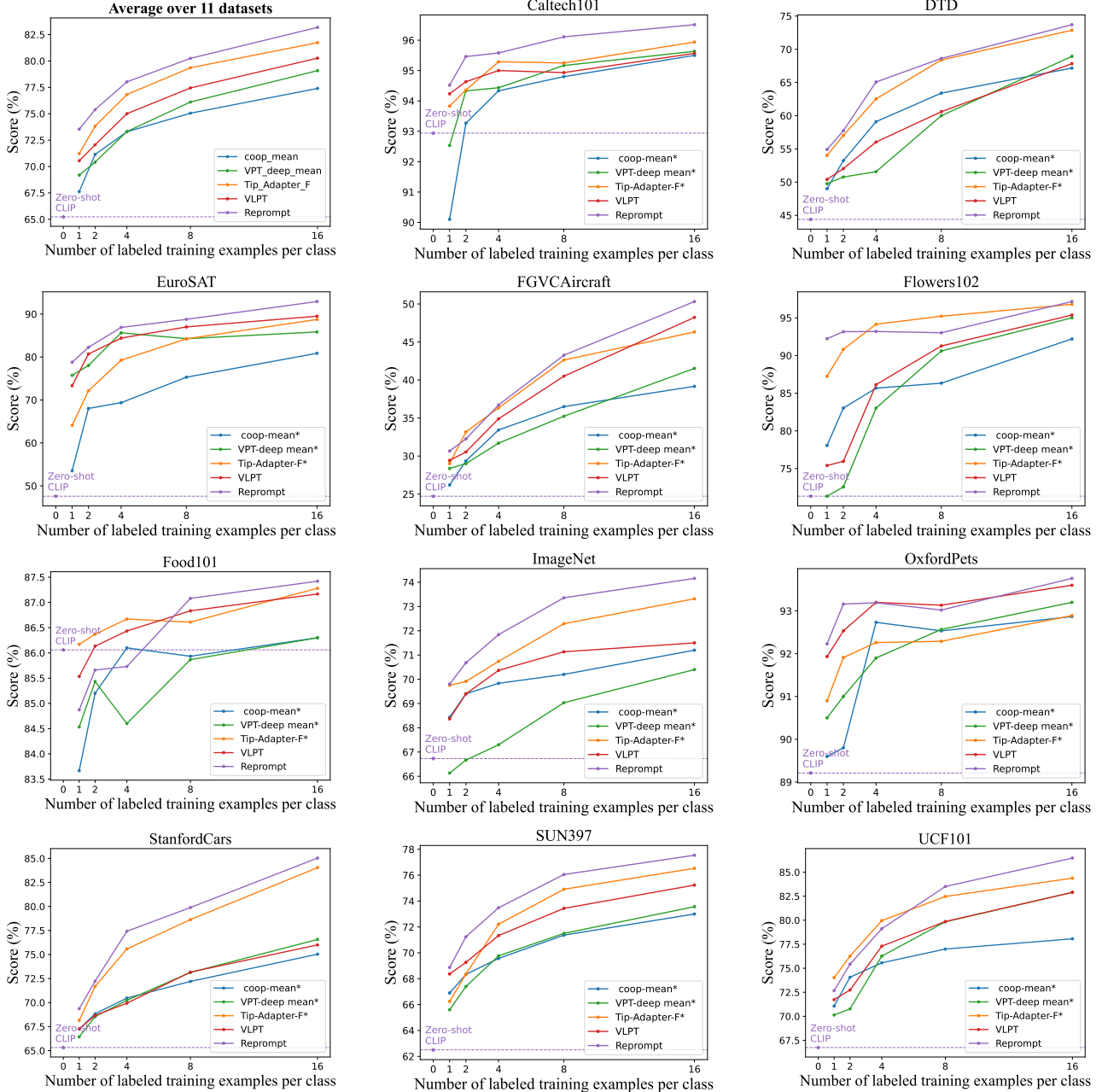


Figure 4. **Main results over 11 datasets under the few-shot settings.** We report the average accuracy(%) of three runs for 1,2,4,8,16 shots. The proposed RePrompt achieves significant performance improvements on most downstream recognition datasets.

loss is formulated as:

$$\mathcal{L} = (1 + \gamma \cdot p_t) \mathcal{L}_{CE}. \quad (9)$$

where  $\gamma$  is a scaling factor. We set  $|\mathbf{K}| = C \times n, n \in \mathbb{N}^*$ . [5] adopts a similar loss for augmenting the model performance on the few-shot learning task of NLP. In few-shot experiments,  $n$  can be 1, 2, 4, 8, 16 to adapt to various few-shot settings.

## 5. Experiments

### 5.1. Few-shot learning

**Datasets.** We evaluate the RePrompt on 11 image classification datasets, including object recognition (ImageNet1k [7] and Caltech101 [9]), fine-grained object recognition (Oxford Pets [37], Flowers102 [36], FGVC-Aircraft [34], Stanford Cars [27] and Food101 [4]), sense recognition (SUN397 [47]), remote sensing recog-

inition(EuroSAT [12]), texture recognition (DTD [6]), and action recognition (UCF101 [43]). To evaluate the performance of RePrompt under few-shot learning settings, we construct 1,2,4,8,16-shot training sets with full categories and the whole test set .

**Baseline.** We compare our proposed RePrompt with four existing prompt-based approaches, namely CoOP [54], VPT-Deep [17], Tip-Adapter-F [51] and VLPT. (1) CoOP learns the context prompt concatenated with [CLASS] as the input of text encoder. (2) VPT-Deep inserts some learnable visual prompts into every transformer layer of the visual encoder. (3) Vision-language prompt tuning (VLPT) jointly optimizes prompts across different modality encoders following CoOP and VPT-Deep. (4) Tip-Adapter-F constructs a cache-model-based adapter from few-shot training data. It can be seen as only interpolating the kNN classifier predictions with the CLIP classification results.

**Training details.** Since prompt tuning is a concept originally introduced in NLP, we naturally extended this concept to unified visual and language models by implementing it on a ViT model, such as ViT-B/16, which is composed of 12 transformer layers like the text encoder. We follow the data preprocessing protocol of CLIP and freeze parameters inherited from the pre-trained model during training. We set hyper-parameters of retrieval modules as following:  $k_{re}$  is 7 and there are 9 random randomly initialized prompts.  $n$  is 8 that resulting in retrieving  $C \times 8$  objects in retrieval-guiding loss. The vision transformer layers equipped with retrieval-enhanced prompts are first 7 layers.

It is worth mentioning that the main experiment was conducted using a single set of hyper-parameters for training and validation. More training details on all datasets and retrieval-result visualization can be found in appendix A and C.

**Results.** The performance of baseline approaches and our proposed RePrompt for few-shot image classification is presented in Figure 4. Our RePrompt consistently superior previous best baselines by +2.32/+1.57/+1.20/+0.89/+1.48 (%) average accuracy on 1/2/4/8/16 shots settings. Based on VLPT, RePrompt achieves significant performance improvement, especially +5.87% on DTD and +9.04% on Stanford Cars. RePrompt greatly boost performance over CoOP and VPT-Deep on challenging datasets with rich categories, such as ImageNet with 1000 classes and SUN397 with 397 classes. We also observe that RePrompt achieves less improvements on Oxford Pets and Food101. This may be caused by noisy data in these datasets [54, 4, 50].

## 5.2. Domain generalization

Pre-trained vision-language models, like CLIP, have strong domain generalization ability. We evaluate the robustness of proposed RePrompt on out-of-distribution (OOD) datasets.

**Datasets.** We follow CoOp [54] and use five datasets, namely, ImageNet, ImageNet V2 [40], ImageNet-Sketch [46], ImageNet-A [14] and ImageNet-R [13]), to evaluate the generalization ability of RePrompt for out-of-distribution (OOD) data. As per the protocol, we train the model over ImageNet (source dataset) on 16-shot setting and evaluate it on other domain shifted datasets (target datasets). Therefore, we use the retrieval database of the ImageNet 16-shot experiment as the retrieval database for target datasets.

**Results.** Table 1 summarizes the OOD experiment results wherein we report the accuracy on both source dataset and target datasets. RePrompt achieves optimal results on ImageNet V2 and ImageNet-R and demonstrates comparable performance with UPT [50] on Image-Sketch. These results demonstrates that RePrompt is a reasonable and more robust approach for prompt tuning.

Methods	ImageNet	V2[40]	S [46]	A [14]	R[13]
CoOP [54]	71.51	64.20	47.99	49.71	75.21
CoCoOP [53]	71.02	64.07	<b>48.75</b>	50.63	76.18
UPT [50]	72.63	64.35	48.66	<b>50.66</b>	76.24
RePrompt	<b>74.62</b>	<b>66.72</b>	48.61	49.48	<b>76.86</b>

Table 1. Main results under the domain generalization setting. We report the average accuracy (%) of 16 shots over three runs.

## 5.3. Ablation

**Component ablation.** We investigate the effectiveness of RePrompt and report results in Table 2. The average accuracy of RePrompt is steadily improved by the gradual introduction of retrieval augmentation modules (+Retrieval-guiding training (+Rg training loss), +Retrieval-enhanced visual prompt (+Re visual prompt),+Retrieval-based adapter (+Rb adapter)).

**Retrieval parameters ablation.** Besides, We presents an experiments on ImageNet to verify the impact of the retrieval in general. Table 3 show that  $k_{re} = 7$  achieves slightly better average performance. The retrieval-enhanced prompt are mainly affected by the convolution kernel size of ReConv. The result under 1-shot setting shows retrieval-enhanced prompts may learn the commonality of similar classes. As shown in Table 4,  $n$  is properly set to be 8,4,4,2,1 on the 16,8,4,2,1-shot settings. A reasonable degree of KNN-guiding training varies in various few-shot settings. Further ablation experiments can be found in appendix B.

**Discussions on ReConv.** We discuss the impact of the network structure used to fuse tokens and queries on the final results of the ReConv model. To this end, we conduct an additional experiment on ImageNet, in which we replace the convolution layer in ReConv. ReRNN is a variant that replaces the convolution layer with an LSTM[15, 41] layer. ReMLP is a variant that replaces the convolution layer with

Method	EuroSAT	Caltech101	Flowers102	Food101	FGVCAircraft	DTD	OxfordPets	StanfordCars	UCF101	SUN397	ImageNet	average
CoOP* [54]	80.87	95.50	92.20	86.30	32.57	67.17	92.87	75.03	78.07	73.00	71.20	76.80
VPT-deep*[17]	85.83	95.63	95.00	86.30	41.53	68.93	93.20	76.57	82.90	73.57	70.40	79.80
Tip-Adapter-F*[51]	88.74	95.94	96.79	87.28	46.32	72.87	92.89	84.04	84.38	76.53	73.32	81.74
VLPT	89.50	95.57	95.37	87.17	48.04	67.83	93.60	76.00	82.90	74.20	71.42	80.14
+Rg training loss	92.48	96.55	94.72	<b>87.56</b>	47.94	69.74	93.54	74.18	83.53	75.20	72.00	80.68
+Re visual prompt	92.60	<b>96.55</b>	95.05	87.48	45.15	69.1	93.62	79.03	82.74	75.6	72.2	80.83
+Rb adapter	<b>92.91</b>	96.51	<b>97.16</b>	87.42	<b>50.32</b>	<b>73.7</b>	<b>93.76</b>	<b>85.04</b>	<b>86.47</b>	<b>77.54</b>	<b>74.62</b>	<b>83.22</b>

Table 2. Component ablation studies over 11 datasets with 16-shot setting. The average accuracy of RePrompt has been steadily improved through the gradual introduction of retrieval enhancement modules.

$k_{re}+2$	16-shot	8-shot	4-shot	2-shot	1-shot	Ave.
2+2	74.50	73.23	<b>71.51</b>	<b>70.53</b>	69.46	71.85
7+2	<b>74.53</b>	<b>73.28</b>	71.38	70.40	<b>69.87</b>	<b>71.89</b>
14+2	74.40	73.11	71.29	70.35	69.64	71.76

Table 3. Ablation study on different visual prompt number over ImageNet with few-shot settings. The retrieval-enhanced prompt are mainly affected by the convolution kernel size of REConv.

$n$	16-shot	8-shot	4-shot	2-shot	1-shot
16	74.30	—	—	—	—
8	<b>74.53</b>	73.11	—	—	—
4	74.26	<b>73.30</b>	<b>71.52</b>	—	—
2	74.31	73.16	71.50	<b>70.40</b>	—
1	74.37	73.23	71.24	70.38	<b>70.02</b>

Table 4. Ablation studies on retrieving  $n$  samples for each class over ImageNet with few-shot settings. The  $k$ NN-guiding training is weak in low-shot settings, since the model may require reference on  $k$ -nn classifier.

a multi-layer perceptron layer. In addition, ReConv( $z_q$ ) is a variant that only takes  $z_q$  as input. The experimental setup for these variants is consistent with that of ReConv, and the number of parameters is controlled to be similar in both models.

method	16-shot	8-shot	4-shot	2-shot	1-shot
ReMLP	74.21	73.02	71.40	70.33	69.50
ReRNN	74.27	72.60	71.12	70.32	69.49
ReConv( $z_q$ )	74.34	72.51	70.84	70.42	69.33
Reconv	<b>74.62</b>	<b>773.36</b>	<b>71.84</b>	<b>70.68</b>	<b>69.87</b>

Table 5. Ablations of ReConv in the visual prompt learner. ReConv demonstrates slightly better performance compared to alternative methods.

As can be seen in Table 5, ReConv achieves slightly better performance compared to others across all shot levels. These results suggest that the specific network structure used to fuse tokens and queries may not have a significant impact on the overall model’s performance. The choice

of network structure may affect the computational cost and optimization difficulty of the model, especially as the complexity of the task increases.

**Training and inference Time.** The performance comparison between all existing methods is listed in Table 6, including training time and inference speed for 16-shot classification on ImageNet. “Wo Retrieval” is a comparable model with the same number of learnable parameters as RePrompt. The results demonstrate that RePrompt achieves a remarkable performance enhancement of 2.71% compared to “Wo Retrieval”. Furthermore, we reduces the training time to just 20 epochs, as opposed to COOP. Considering the trade-off between accuracy improvement and inference speed, we believe that the inference speed is acceptable for few-shot image classification.

Methods	Acc.(%)	Param.(M)	Train.	Epochs	Inf.(ms)
COOP	71.20	0.4	14h40min	200	299.64
Tip-Adapter-F	73.32	8.19	5min	20	10.5
VLPT	71.42	0.45	15h50min	100	214.84
RePrompt	74.62	11.11	4h	20	262.57
Wo Retrieval	71.91	11.11	3h30min	20	215.20

Table 6. Comparison of classification accuracy and time efficiency for different methods on 16-shot ImageNet. All experiments are trained with batch 16 and tested with batch size 32.

## 5.4. Visualization of Manifold

To highlight the impact of retrieval-enhanced prompts on the visual features, we employ t-SNE [39] to visualize the manifold of CLIP, VLPT, and RePrompt models after training on the EuroSAT dataset. The t-SNE visualization results are presented in Figure 5. It is clearly illustrated that in high-dimensional classification space, RePrompt shows much more distinct separation of image features (with feature distributions more parallel to the z-axis) belonging to different categories. The retrieval-based adapter leverages these features as inputs and produces superior classification results, thereby significantly enhancing the final classification outcome.



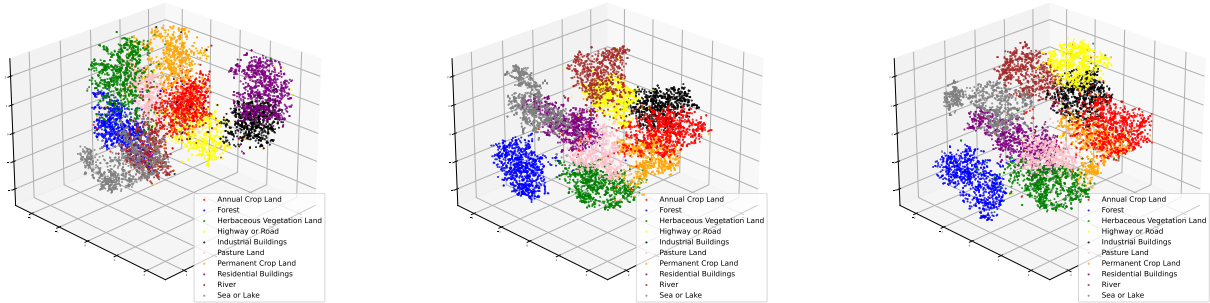


Figure 5. Visualization of different learned visual feature manifolds via t-SNE.

## 6. Conclusion

In this paper, we presented RePrompt, a novel retrieval-based framework that enhances the performance of prompt learning methods on few-shot classification tasks. Our proposed method consists of a retrieval-based adapter and retrieval-enhanced prompts to augment the different stages of a simple prompt learning baseline. Extensive experiment results show that the proposed method achieves superior performance among other prompt-learning methods in few-shot learning and comparable results on domain-generalization.

We hope that our work inspires further research in these noteworthy directions: 1) extend prompt learning to other downstream tasks, such as segmentation, 2) explore retrieval to solve other problems, e.g., long-tail classification.

**Acknowledgement** This work was supported by National Key R&D Program of China (No. 2022ZD0118700) and Natural Science Foundation of Zhejiang Province (NO. LY21F030018).

## Appendix

This supplementary material provides additional implementation details (in A), further retrieval impact analysis (in B), retrieval visualization (in C) and dataset introduction (in D).

### A. Additional implementation details

This section provides more experimental details, include training settings and approach design settings.

Table 7 demonstrates more training hyper-parameters. For the few-shot setting on ImageNet, training epoch is set to 20 to relieve the overfitting. We also increase the training epoch to 100 on FGVC Aircraft and EuroSAT for salient performance improvements. The train epoch is set to 50

for other datasets. Experiments on a single dataset are conducted using a single 3090 GPU. Limited by GPU memory, we set the batch size to 64 for ImageNet and 128 for other datasets. We fine-tune the prompt and adapter using the AdamW optimizer with a learning rate of  $1e-3$  and an epsilon value of  $1e-4$ . Other data preprocess settings and training settings are the default parameters of CoOP [54].

Table 8 summarizes key factors in the our proposed RePrompt approach, e.g.,  $\lambda$ . The value of  $n$  is verified as 8,4,4,2,1 in 16,8,4,2,1 shot.  $\lambda$  varies with downstream tasks changing. Thus, we provide only a mean value across all downstream tasks.  $\beta$  is set to 10 to scale up the output of REConv.  $k_{re}$  denotes the number of retrieved representations that are used to generate  $k_{re}+2$  visual prompts. Hyper-parameter details for prompt learning variants are presented in Table 12. In RePrompt, "12/1/7" means that visual prompt depth is 12 and text prompt depth is 1. Besides, "7" represents that we add 7 collections of retrieval-enhanced prompts on the first 7 visual prompt sets.

Training hyper-parameter	Value
Training epoch	{50, 100, 20}
Batch size	{128, 64}
Learning rate	$1e-3$
Optimizer	adamw
Adam epsilon	$1e-4$

Table 7. Training hyper-parameter settings of the RePrompt on various datasets.

Approach hyper-parameter	Value
$n$	{8, 4, 4, 2, 1}
$\lambda$	0.5
$\gamma$	$1e-4$
$\beta$	10
$k_{re}$	7

Table 8. Approach hyper-parameter settings of the RePrompt on ImageNet-1k.

## B. More ablation

Since the retrieval database derived from training data in the few-shot setting, the performance improvements of RePrompt are closely related to data statistics. We further study the correlation between the performance improvement of our method and the intra-class variance of visual feature. The specific correlation is visualized in Figure 6, which represents the relationship between intra-class visual variance and the performance improvement achieved by the three-part stepwise overlay of RePrompt.

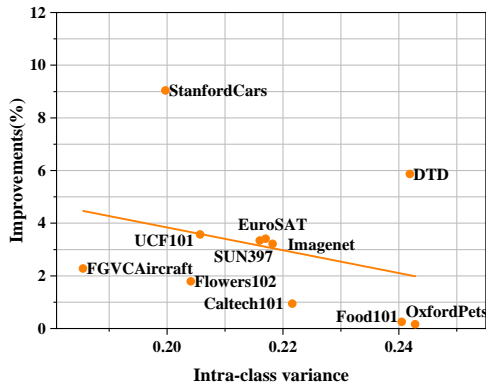


Figure 6. **Visualization results** of the correlation between performance improvements and intra-class visual variance. The improvements of RePrompt overall decrease with increasing intra-class visual variance.

### B.1. Intra-class visual variance

This subsection provide the implementation details of calculating the intra-class visual variance and specific variance values of downstream tasks. Given a downstream training dataset with  $C$  classes in total and each class has 16 images, we first use the CLIP image encoder  $e_1$  to extract image features  $z$  for image  $x$ . Then we get the intra-class variance of class  $c$  as:

$$v_c = \frac{1}{\|X_c\|} \sum_{x \in X_c} (z - \bar{z})^2 \quad (10)$$

where  $X_c$  represents the collection of images with ground-truth class label  $c$  and  $\bar{z}$  denotes the mean representation of class  $c$ . Then, the intra-class variance  $\hat{v}$  for all the  $C$  classes of the downstream dataset as:

$$\hat{v} = \frac{1}{C} \sum_{c=1}^C v_c \quad (11)$$

We calculate intra-class visual variances over 11 datasets with 16-shot setting and report values in Table 11.

### B.2. Further Analysis of Retrieval Impact.

We perform two experiments over FGVC Aircraft and Oxford Pets to further quantify the impact of retrieval under various few-shot settings. FGVC Aircraft and Oxford Pets have the smallest and largest inter-class visual variance, respectively. Thus We compare the optimal retrieval parameter adjustments between these datasets to reflect the impact of inter-class visual variance on the retrieval mechanism.

The retrieval-enhanced prompt number  $k_{re} + 2$  increasing represents that RePrompt needs more retrieved information. As shown in Table 9, the optimal  $k_{re}$  parameter varies between the two datasets. In particular, we find that  $k_{re} = 14$  never obtains better performance on Oxford Pets in all few-shot settings, indicating that retrieved information is negative and low-confidence on datasets with high inter-class visual variance. However,  $k_{re} = 14$  achieves better average performance on FGVC Aircraft.

$k_{re}+2$	Dataset	16-shot	8-shot	4-shot	2-shot	1-shot	Ave
2+2	FGVC Aircraft	53.05	45.84	39.39	34.86	31.05	40.838
7+2		54.61	47.94	40.05	35.61	<b>31.23</b>	41.888
14+2		<b>54.91</b>	<b>47.97</b>	<b>40.17</b>	<b>35.79</b>	31.17	<b>42.002</b>
2+2	Oxford Pets	94.58	<b>93.84</b>	93.21	<b>92.97</b>	91.55	93.23
7+2		<b>94.85</b>	93.57	<b>93.62</b>	92.94	<b>91.82</b>	<b>93.36</b>
14+2		94.47	93.65	93.16	93.21	91.41	93.18

Table 9. Ablation study on different visual prompt number over Fgvc Aircraft and Oxford Pets with few-shot settings. The retrieval-enhanced prompt are mainly affected by the convolution kernel size of REConv.

The factor  $n$  controls the retrieval  $C \times n$  samples in retrieval-guiding training loss. A larger value of  $n$  indicates a looser constraint on retrieval. As shown in Table 10,  $n = 1$  achieves optimal performance in 16-shot setting on Oxford Pets, which implies RePrompt prefers the output of CLIP with retrieval-enhanced prompt. However, in low-shot scenarios(e.g.,  $n = 2/1$  under 2/1-shot setting), RePrompt may require more reference since there is no sufficient data for training.

$n$	Dataset	16-shot	8-shot	4-shot	2-shot	1-shot
16	FGVC Aircraft	54.40	—	—	—	—
8		54.61	<b>47.94</b>	—	—	—
4		<b>54.79</b>	47.28	<b>40.11</b>	—	—
2		54.04	47.31	39.96	<b>35.81</b>	—
1		54.58	47.31	40.05	35.43	<b>31.23</b>
16	Oxford Pets	94.60	—	—	—	—
8		94.49	93.43	—	—	—
4		94.55	<b>93.57</b>	<b>93.62</b>	—	—
2		94.69	93.51	93.21	<b>92.94</b>	—
1		<b>94.85</b>	93.46	93.57	92.70	<b>91.82</b>

Table 10. Ablation studies on retrieving  $n$  samples for each class over Fgvc Aircraft and Oxford Pets with few-shot settings. The  $k$ NN-guiding training is weak in low-shot settings, since the model may require reference on  $k$ -nn classifier.

**Based on the above analysis, we summarize two empirical rules as follows:** 1) For a dataset with low/high

intra-class visual variance, we should enable the retrieval model that has a strong/weak ability to ensure a stable overall performance improvement. 2) In low-shot setting, inference results mainly depend on retrieval results.

### B.3. Tuning retrieval parameters.

The final distribution of the prediction in RePrompt is affected by the hyper-parameters of  $\gamma$  and  $\lambda$ , as well as the retrieval-enhanced prompt depth  $J$ . We conduct ablation experiments to explore the effects of these hyper-parameters on the final results over various datasets.

As shown in Figure 7, from top to bottom, ablation experiments are carried out on FGVC Aircraft, ImageNet, and Oxford Pets under the 16-shot learning setting. We follow the default settings in the above experiments on ImageNet, except for changing depth  $J$ ,  $\gamma$  and  $\lambda$ .

**$\lambda$  varies.** The hyper-parameter  $\lambda$  controls how much to combine predictions from the adapter, which can be interpreted as weighting the CLIP with the learned prompt and the  $k$ -nn classifier. larger  $\lambda$  represents using more knowledge from the retrieval and less otherwise. From the left part in Figure 7, we observe that the performance improves overall, as  $\lambda$  increases from 0.0 to 0.7, achieving the best accuracy, 54.61% on FGVC Aircraft, 74.64% on ImageNet and 94.55% on Oxford Pets. This finding suggests that RePrompt benefits from using more knowledge from the retrieval on datasets with low intra-class visual variance. However, this conclusion may not hold in datasets with high intra-class visual variance.

**$J$  varies.** Depth  $J$  denotes the insertion depth of retrieval-enhanced prompt, which can be seen as a metric that represents the degree of retrieval participating in the prompt learning. From the medium part of Figure 7, we find that a moderate insertion depth of retrieval-enhanced prompt is optimal, 54.91% at the first 5 layers on FGVC Aircraft, 74.57% at the first 3 layers on ImageNet, and 94.58% at the first 6 layers on Oxford Pets. The finding highlights that a moderate depth of retrieval-enhanced prompt is essential since retrieved representations can introduce additional information, but excessive attendance of retrieval also can bring noise.

**$\gamma$  varies.**  $\gamma$  in the guiding loss  $\mathcal{L}$  controls the hardness of the retrieval. large  $\gamma$  forces the retrieval to have a weak effect on final results. As shown in the right part of Figure 7, the result continues to improve as  $\gamma$  decreases. It illustrates that a retrieval augmentation is effective to ensure classification accuracy improvements.

In summary, the hyper-parameters of retrieval play a critical role in achieving optimal performance in retrieval-enhanced methods. These findings highlight the importance of balancing the amount of additional information retrieved and the introduction of noise in the learning process. It provides insights into the design and optimization of related

methods and can guide future research in this field.

## C. Retrieval visualization

To intuitively show the effect of our retrieval mechanism and influence of various  $e_R$ , we also present some retrieved images for query samples in Figure 8. The visualization result demonstrates that retrieval can search similar samples and the image encoder of CLIP is a better  $e_R$  to find more correct images.

## D. Datasets

The details of the 11 downstream datasets for few-shot classification and 4 target datasets for domain generalization are shown in Table 13.

Method	FGVCAircraft	StanfordCars	Flowers102	UCF101	SUN397	EuroSAT	ImageNet	Caltech101	Food101	DTD	OxfordPets
Intra-class variance	<b>0.186</b>	0.200	0.204	0.206	0.216	0.217	<b>0.218</b>	0.222	0.241	0.242	<b>0.243</b>

Table 11. Intra-class visual variance over 11 datasets under the 16-shot learning setting. The variance progressively increases from left to right.

Method	Depth(Visual/Text/Retrieval-enhanced)	Visual prompt number	Text prompt number(Initial Prompt)
CoOP [54]	0/1/0	0	4("a photo of a")
VPT-deep [17]	12/0/0	9	0("a photo of a")
VLPT	12/1/0	9	4("a photo of a")
RePrompt	12/1/7	9	4("a photo of a")

Table 12. Hyper-parameter settings of prompt learning variants. Depth denotes the prompt inserted depth."a photo of a" is the initial text prompt.

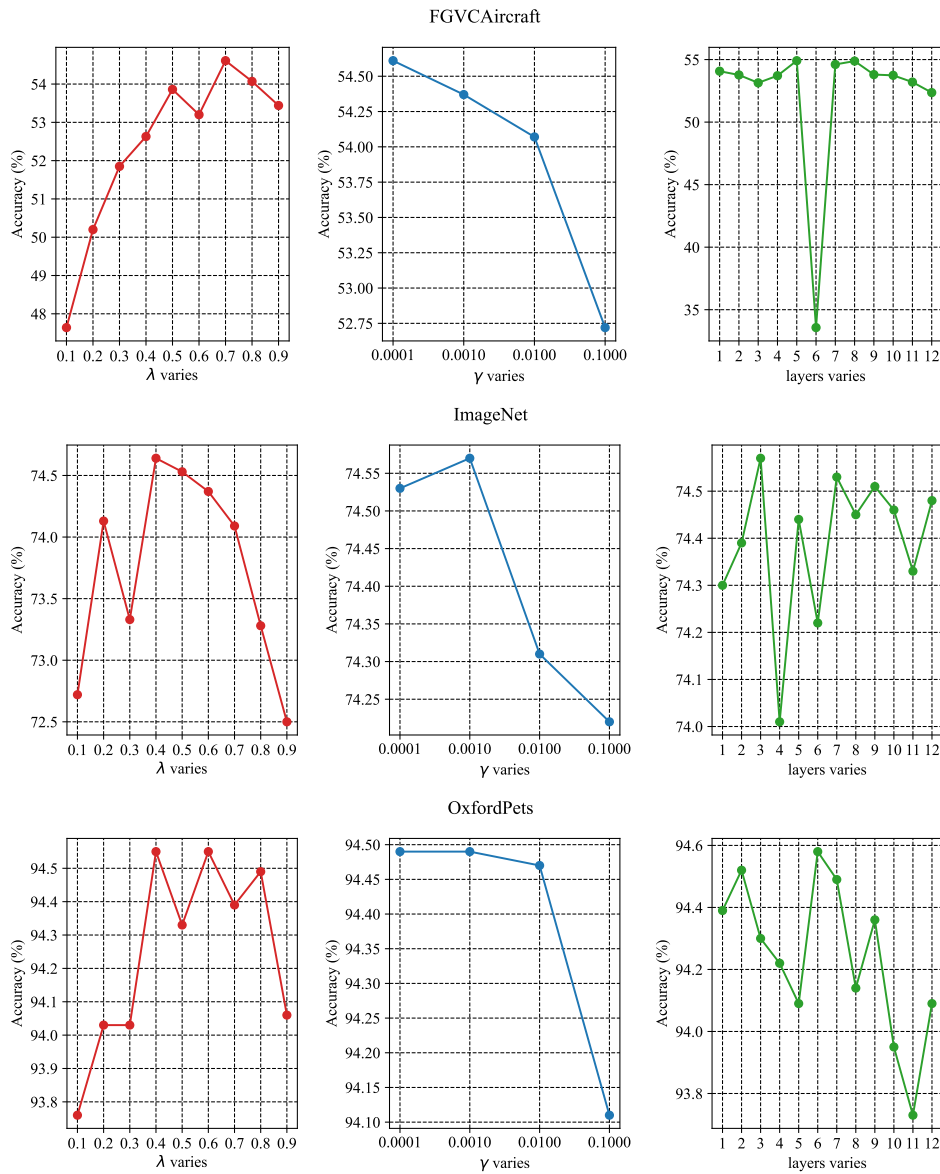


Figure 7. Tuning retrieval parameter results over 3 datasets under the 16-shot learning setting. From top to bottom, images report ablation experiments about tuning retrieval parameters on FGVC Aircraft, ImageNet and Oxford Pets, respectively.

Dataset	Type	Classes	Test Size
ImageNet [7]	object recognition	1000	50000
Sun397 [47]	sense recognition	397	19850
Food101 [4]	food recognition	101	30300
Stanford Cars [27]	fine-grained object recognition	196	8041
FGVC Aircraft [34]	fine-grained object recognition	100	3333
Oxford Pets [37]	fine-grained object recognition	37	3669
Oxford Flowers [36]	fine-grained object recognition	102	2463
Caltech-101 [9]	object recognition	100	2465
EuroSAT [12]	remote sensing recognition	10	8100
UCF-101 [43]	action recognition	101	3783
Describable Textures(DTD) [6]	texture recognition	47	1692
ImageNetV2 [40]	N/A	1000	10000
ImageNet-Sketch [46]	N/A	1000	50889
ImageNet-A [14]	N/A	200	7500
ImageNet-R [13]	N/A	200	30000

Table 13. Dataset details in our experiments.



Figure 8. Examples of the retrieval mechanism using various  $e_R$  on ImageNet with the 16-shot setting. ViT-B/16 (Image encoder of CLIP) means that  $e_R$  adopts ViT-B/16 trained by CLIP. ViT-B/16(Timm) denotes that  $e_R$  adopts ViT-B/16 trained by Timm under full supervision. Top  $k$  means the  $k$  nearest neighbor and IPS. denotes the inner product similarity. The image encoder of CLIP as  $e_R$  to participate in retrieval can get more similar and correct images, especially for some hard samples, such as "velvet fabric".

## References

- [1] Andreas Blattmann, Robin Rombach, Kaan Oktay, and Björn Ommer. Retrieval-augmented diffusion models. *arXiv preprint arXiv:2204.11824*, 2022.
- [2] Gianluca Bontempi, Hugues Bersini, and Mauro Birattari. The local paradigm for modeling and control: from neuro-fuzzy to lazy learning. *Fuzzy sets and systems*, 121(1):59–72, 2001.
- [3] Sebastian Borgeaud, Arthur Mensch, Jordan Hoffmann, Trevor Cai, Eliza Rutherford, Katie Millican, George Bm Van Den Driessche, Jean-Baptiste Lespiau, Bogdan Damoc, Aidan Clark, et al. Improving language models by retrieving from trillions of tokens. In *ICML*, pages 2206–2240, 2022.
- [4] Lukas Bossard, Matthieu Guillaumin, and Luc Van Gool. Food-101—mining discriminative components with random forests. In *ECCV*, pages 446–461, 2014.
- [5] Xiang Chen, Lei Li, Ningyu Zhang, Xiaozhuan Liang, Shumin Deng, Chuanqi Tan, Fei Huang, Luo Si, and Huajun Chen. Decoupling knowledge from memorization: Retrieval-augmented prompt learning. *arXiv preprint arXiv:2205.14704*, 2022.
- [6] Mircea Cimpoi, Subhansu Maji, Iasonas Kokkinos, Sammy Mohamed, and Andrea Vedaldi. Describing textures in the wild. In *CVPR*, pages 3606–3613, 2014.
- [7] Jia Deng, Wei Dong, Richard Socher, Li-Jia Li, Kai Li, and Li Fei-Fei. Imagenet: A large-scale hierarchical image database. In *CVPR*, pages 248–255, 2009.
- [8] Alexey Dosovitskiy, Lucas Beyer, Alexander Kolesnikov, Dirk Weissenborn, Xiaohua Zhai, Thomas Unterthiner, Mostafa Dehghani, Matthias Minderer, Georg Heigold, Sylvain Gelly, et al. An image is worth 16x16 words: Transformers for image recognition at scale. *arXiv preprint arXiv:2010.11929*, 2020.
- [9] Li Fei-Fei, Rob Fergus, and Pietro Perona. Learning generative visual models from few training examples: An incremental bayesian approach tested on 101 object categories. In *CVPR*, pages 178–178, 2004.
- [10] Chelsea Finn, Pieter Abbeel, and Sergey Levine. Model-agnostic meta-learning for fast adaptation of deep networks. In *ICML*, pages 1126–1135, 2017.
- [11] Kelvin Guu, Kenton Lee, Zora Tung, Panupong Pasupat, and Mingwei Chang. Retrieval augmented language model pre-training. In *ICML*, pages 3929–3938, 2020.
- [12] Patrick Helber, Benjamin Bischke, Andreas Dengel, and Damian Borth. Eurosat: A novel dataset and deep learning benchmark for land use and land cover classification. *IEEE Journal of Selected Topics in Applied Earth Observations and Remote Sensing*, 12(7):2217–2226, 2019.
- [13] Dan Hendrycks, Steven Basart, Norman Mu, Saurav Kadavath, Frank Wang, Evan Dorundo, Rahul Desai, Tyler Zhu, Samyak Parajuli, Mike Guo, et al. The many faces of robustness: A critical analysis of out-of-distribution generalization. In *ICCV*, pages 8340–8349, 2021.
- [14] Dan Hendrycks, Kevin Zhao, Steven Basart, Jacob Steinhardt, and Dawn Song. Natural adversarial examples. In *CVPR*, pages 15262–15271, 2021.
- [15] Sepp Hochreiter and Jürgen Schmidhuber. Long short-term memory. *Neural computation*, 9(8):1735–1780, 1997.
- [16] Chao Jia, Yinfei Yang, Ye Xia, Yi-Ting Chen, Zarana Parekh, Hieu Pham, Quoc Le, Yun-Hsuan Sung, Zhen Li, and Tom Duerig. Scaling up visual and vision-language representation learning with noisy text supervision. In *ICML*, pages 4904–4916, 2021.
- [17] Menglin Jia, Luming Tang, Bor-Chun Chen, Claire Cardie, Serge Belongie, Bharath Hariharan, and Ser-Nam Lim. Visual prompt tuning. *arXiv preprint arXiv:2203.12119*, 2022.
- [18] Shibo Jie and Zhi-Hong Deng. Convolutional bypasses are better vision transformer adapters. *arXiv preprint arXiv:2207.07039*, 2022.
- [19] Shibo Jie and Zhi-Hong Deng. Fact: Factor-tuning for lightweight adaptation on vision transformer. *arXiv preprint arXiv:2212.03145*, 2022.
- [20] Jeff Johnson, Matthijs Douze, and Hervé Jégou. Billion-scale similarity search with gpus. *IEEE Transactions on Big Data*, 7(3):535–547, 2019.
- [21] Chen Ju, Tengda Han, Kunhao Zheng, Ya Zhang, and Weidi Xie. Prompting visual-language models for efficient video understanding. In *ECCV*, pages 105–124, 2022.
- [22] Vladimir Karpukhin, Barlas Oğuz, Sewon Min, Patrick Lewis, Ledell Wu, Sergey Edunov, Danqi Chen, and Wen-tau Yih. Dense passage retrieval for open-domain question answering. *arXiv preprint arXiv:2004.04906*, 2020.
- [23] Nora Kassner and Hinrich Schütze. Bert-knn: Adding a knn search component to pretrained language models for better qa. *arXiv preprint arXiv:2005.00766*, 2020.
- [24] Urvashi Khandelwal, Omer Levy, Dan Jurafsky, Luke Zettlemoyer, and Mike Lewis. Generalization through memorization: Nearest neighbor language models. *arXiv preprint arXiv:1911.00172*, 2019.
- [25] Muhammad Uzair Khattak, Hanoona Rasheed, Muhammad Maaz, Salman Khan, and Fahad Shahbaz Khan. Maple: Multi-modal prompt learning. *arXiv preprint arXiv:2210.03117*, 2022.
- [26] James Kirkpatrick, Razvan Pascanu, Neil Rabinowitz, Joel Veness, Guillaume Desjardins, Andrei A Rusu, Kieran Milan, John Quan, Tiago Ramalho, Agnieszka Grabska-Barwinska, et al. Overcoming catastrophic forgetting in neural networks. *Proceedings of the national academy of sciences*, 114(13):3521–3526, 2017.
- [27] Jonathan Krause, Michael Stark, Jia Deng, and Li Fei-Fei. 3d object representations for fine-grained categorization. In *ICCV*, pages 554–561, 2013.
- [28] Brian Lester, Rami Al-Rfou, and Noah Constant. The power of scale for parameter-efficient prompt tuning. *arXiv preprint arXiv:2104.08691*, 2021.
- [29] Patrick Lewis, Ethan Perez, Aleksandra Piktus, Fabio Petroni, Vladimir Karpukhin, Naman Goyal, Heinrich Küttler, Mike Lewis, Wen-tau Yih, Tim Rocktäschel, et al. Retrieval-augmented generation for knowledge-intensive nlp tasks. *NeurIPS*, pages 9459–9474, 2020.
- [30] Xiang Lisa Li and Percy Liang. Prefix-tuning: Optimizing continuous prompts for generation. *arXiv preprint arXiv:2101.00190*, 2021.

- [31] Tsung-Yi Lin, Priya Goyal, Ross Girshick, Kaiming He, and Piotr Dollár. Focal loss for dense object detection. In *ICCV*, pages 2980–2988, 2017.
- [32] Alexander Long, Wei Yin, Thalaiyasingam Ajanthan, Vu Nguyen, Pulak Purkait, Ravi Garg, Alan Blair, Chunhua Shen, and Anton van den Hengel. Retrieval augmented classification for long-tail visual recognition. In *CVPR*, pages 6959–6969, 2022.
- [33] Yuning Lu, Jianzhuang Liu, Yonggang Zhang, Yajing Liu, and Xinmei Tian. Prompt distribution learning. In *CVPR*, pages 5206–5215, 2022.
- [34] Subhransu Maji, Esa Rahtu, Juho Kannala, Matthew Blaschko, and Andrea Vedaldi. Fine-grained visual classification of aircraft. *arXiv preprint arXiv:1306.5151*, 2013.
- [35] Kengo Nakata, Youyang Ng, Daisuke Miyashita, Asuka Maki, Yu-Chieh Lin, and Jun Deguchi. Revisiting a knn-based image classification system with high-capacity storage. *arXiv preprint arXiv:2204.01186*, 2022.
- [36] Maria-Elena Nilsback and Andrew Zisserman. Automated flower classification over a large number of classes. In *2008 Sixth Indian Conference on Computer Vision, Graphics & Image Processing*, pages 722–729, 2008.
- [37] Omkar M Parkhi, Andrea Vedaldi, Andrew Zisserman, and CV Jawahar. Cats and dogs. In *CVPR*, pages 3498–3505, 2012.
- [38] Alec Radford, Jong Wook Kim, Chris Hallacy, Aditya Ramesh, Gabriel Goh, Sandhini Agarwal, Girish Sastry, Amanda Askell, Pamela Mishkin, Jack Clark, et al. Learning transferable visual models from natural language supervision. In *ICML*, pages 8748–8763, 2021.
- [39] Alec Radford, Jong Wook Kim, Chris Hallacy, Aditya Ramesh, Gabriel Goh, Sandhini Agarwal, Girish Sastry, Amanda Askell, Pamela Mishkin, Jack Clark, et al. Learning transferable visual models from natural language supervision. In *International conference on machine learning*, pages 8748–8763. PMLR, 2021.
- [40] Benjamin Recht, Rebecca Roelofs, Ludwig Schmidt, and Vaishal Shankar. Do imagenet classifiers generalize to imagenet? In *ICML*, pages 5389–5400, 2019.
- [41] Hasim Sak, Andrew W. Senior, and Françoise Beaufays. Long short-term memory recurrent neural network architectures for large scale acoustic modeling. In *INTERSPEECH*, pages 338–342, 2014.
- [42] Jake Snell, Kevin Swersky, and Richard Zemel. Prototypical networks for few-shot learning. *NeurIPS*, 30, 2017.
- [43] Khurram Soomro, Amir Roshan Zamir, and Mubarak Shah. Ucf101: A dataset of 101 human actions classes from videos in the wild. *arXiv preprint arXiv:1212.0402*, 2012.
- [44] Mariya Toneva, Alessandro Sordani, Remi Tachet des Combes, Adam Trischler, Yoshua Bengio, and Geoffrey J Gordon. An empirical study of example forgetting during deep neural network learning. *arXiv preprint arXiv:1812.05159*, 2018.
- [45] Oriol Vinyals, Charles Blundell, Timothy Lillicrap, Daan Wierstra, et al. Matching networks for one shot learning. *NeurIPS*, 29, 2016.
- [46] Haohan Wang, Songwei Ge, Zachary Lipton, and Eric P Xing. Learning robust global representations by penalizing local predictive power. *NeurIPS*, 32, 2019.
- [47] Jianxiong Xiao, James Hays, Krista A Ehinger, Aude Oliva, and Antonio Torralba. Sun database: Large-scale scene recognition from abbey to zoo. In *CVPR*, pages 3485–3492, 2010.
- [48] Yinghui Xing, Qirui Wu, De Cheng, Shizhou Zhang, Guoqiang Liang, and Yanning Zhang. Class-aware visual prompt tuning for vision-language pre-trained model. *arXiv preprint arXiv:2208.08340*, 2022.
- [49] Zhuolin Yang, Wei Ping, Zihan Liu, Vijay Korthikanti, Weili Nie, De-An Huang, Linxi Fan, Zhiding Yu, Shiyi Lan, Bo Li, et al. Re-vilm: Retrieval-augmented visual language model for zero and few-shot image captioning. *arXiv preprint arXiv:2302.04858*, 2023.
- [50] Yuhang Zang, Wei Li, Kaiyang Zhou, Chen Huang, and Chen Change Loy. Unified vision and language prompt learning. *arXiv preprint arXiv:2210.07225*, 2022.
- [51] Renrui Zhang, Wei Zhang, Rongyao Fang, Peng Gao, Kunchang Li, Jifeng Dai, Yu Qiao, and Hongsheng Li. Tip-adapter: Training-free adaption of clip for few-shot classification. In *ECCV*, pages 493–510, 2022.
- [52] Yuanhan Zhang, Kaiyang Zhou, and Ziwei Liu. Neural prompt search. *arXiv preprint arXiv:2206.04673*, 2022.
- [53] Kaiyang Zhou, Jingkang Yang, Chen Change Loy, and Ziwei Liu. Conditional prompt learning for vision-language models. In *CVPR*, pages 16816–16825, 2022.
- [54] Kaiyang Zhou, Jingkang Yang, Chen Change Loy, and Ziwei Liu. Learning to prompt for vision-language models. *IJCV*, 130(9):2337–2348, 2022.